



Published in final edited form as:

Angiogenesis. 2020 November ; 23(4): 685–698. doi:10.1007/s10456-020-09740-y.

IQGAP1 Causes Choroidal Neovascularization by Sustaining VEGFR2-mediated Rac1 Activation

Haibo Wang¹, Aniket Ramshekar¹, Eric Kunz¹, David B Sacks², M. Elizabeth Hartnett^{1,*}

¹The John A Moran Eye Center, University of Utah, Salt Lake City, UT

²Department of Laboratory Medicine, National Institutes of Health, Bethesda, Maryland 20892

Abstract

Loss of visual acuity in neovascular age-related macular degeneration (nAMD) occurs when factors activate choroidal endothelial cells (CECs) to transmigrate the retinal pigment epithelium into the sensory retina and develop into choroidal neovascularization (CNV). Active Rac1 (Rac1GTP) is required for CEC migration and is induced by different AMD-related stresses, including vascular endothelial growth factor (VEGF). Besides its role in pathologic events, Rac1 also plays a role in physiologic functions. Therefore, we were interested in a method to inhibit pathologic activation of Rac1. We addressed the hypothesis that IQGAP1, a scaffold protein with a Rac1 binding domain, regulates pathologic Rac1GTP in CEC migration and CNV. Compared to littermate *Iqgap1*^{+/+}, *Iqgap1*^{-/-} mice had reduced volumes of laser-induced CNV and decreased Rac1GTP and phosphorylated VEGFR2 (p-VEGFR2) within lectin-stained CNV. Knockdown of IQGAP1 in CECs significantly reduced VEGF-induced Rac1GTP, mediated through p-VEGFR2, which was necessary for CEC migration. Moreover, sustained activation of Rac1GTP induced by VEGF was eliminated when CECs were transfected with an IQGAP1 construct that is unable to bind Rac1. IQGAP1-mediated Src activation was involved in initiating Rac1 activation, CEC migration and tube formation. Our findings indicate that in CECs IQGAP1 interacts with VEGFR2 to mediate Src activation and subsequent Rac1 activation and CEC migration. In addition, IQGAP1 binding to Rac1GTP results in sustained activation of Rac1, leading to CEC migration toward VEGF. Our study supports a role of IQGAP1 and the interaction between IQGAP1 and Rac1GTP to restore CECs quiescence and, therefore, prevent vision-threatening CNV in nAMD.

*Correspondence to: M. Elizabeth Hartnett, MD, Address: 65 Mario Capecchi Drive, Salt Lake City, UT 84132., Tel: 801-213-4110; Fax: 801-581-3357, ME.Hartnett@hsc.utah.edu.

Authors' contributions

HW designed and performed the experiments and wrote the manuscript; AR and EK performed experiments and house the animals; DBS provided the animals, reagents and wrote the manuscript; MEH designed the experiments, wrote the manuscript and provided funding supports.

Publisher's Disclaimer: This Author Accepted Manuscript is a PDF file of an unedited peer-reviewed manuscript that has been accepted for publication but has not been copyedited or corrected. The official version of record that is published in the journal is kept up to date and so may therefore differ from this version.

Conflicts of Interests

The authors declared there were no conflicts of interests to disclose.

Keywords

Age-related macular degeneration; choroidal neovascularization; IQGAP1; Vascular endothelial growth factor; Vascular endothelial growth factor receptor 2; Rac1

Introduction

Age-related macular degeneration (AMD) is a leading cause of vision loss worldwide [1]. Loss in visual acuity occurs rapidly in neovascular AMD when various stresses and factors activate choroidal endothelial cells (CECs) and overwhelm homeostatic mechanisms that prevent CEC transmigration of the retinal pigment epithelium (RPE) [2]. Once in the subretinal space, CECs can proliferate and develop into choroidal neovascularization (CNV), which is called type 2 neovascularization as it resides in the space between the photoreceptor outer segments and the RPE and distinguished it from type 1 (beneath the RPE) and type 3 (within the retina) neovascularization [3]. Studies from human clinical trials support early findings that CNV beneath the RPE (type 1 neovascularization) may be inactive and asymptomatic and potentially support the outer retina with oxygen, nutrients and by removing waste products [2, 4]. In contrast, active CNV within the subretinal space is believed to cause vision loss from leakage of fluid within and beneath the retina and from later fibrovascular proliferation [5–7]. CEC activation and migration would require the coordination of multiple cell events, for example, cytoskeletal reorganization and activation and translocation of the GTPase, active Rac1 (Rac1GTP), to the plasma membrane to increase cell motility [8–10]. We previously provided evidence that Rac1GTP was necessary for CEC transmigration of an RPE monolayer [11] and that many signaling mechanisms involved in the pathophysiology of neovascular AMD activate Rac1, including through inflammatory (e.g., tumor necrosis factor alpha, TNF α), angiogenic (e.g., vascular endothelial growth factor, VEGF), and oxidative (e.g., NADPH oxidase-generated ROS) pathways [12–14].

Rac1 is a member of the Rho-family of GTPases and plays important roles in several diseases by acting as a biologic switch. Rac1 is activated by a variety of guanine nucleotide exchange factors (GEFs) that cause it to be GTP-bound (Rac1GTP) and inactivated by GTPase activating proteins (GAPs) that enhance hydrolysis of GTP to GDP (Rac1GDP) [15, 16]. Rac1GTP can lead to biologic outcomes, including cytoskeletal remodeling and cell motility. Finding a general inhibitor of Rac1 would seem an effective treatment for neovascular AMD by interfering with CEC activation and migration. However, evidence suggests total inhibition of Rac1 may be detrimental: Rac1 knockout is lethal, potentially because Rac1 has physiologic functions, particularly in fighting microbes [17, 18]. Also, inhibitors against specific GEFs that induce Rac1 activation are poorly effective in angiogenic diseases, potentially because Rac1 is activated by many different GEFs [19, 20]. Thus, a safe therapeutic approach that dampens the many signaling mechanisms that activate Rac1 in CECs may be an effective strategy to treat neovascular AMD safely.

IQ protein motif containing GTPase activating protein 1 (IQGAP1) is a highly conserved, RasGAP-related, multi-domain scaffolding protein [21–23]. IQGAP1 affects cell physiology

by binding partners, enabling complex cell and biologic events that link signaling pathways. By binding to different proteins, IQGAP1 integrates multiple signaling effectors within the cell, such as F-actin, Rac1, Cdc42, ERK, Rap1 and calmodulin, to modulate the actin cytoskeleton and enable cell motility, as an example. The specific binding of Rac1GTP to the GAP-related domain (GRD) of IQGAP1 has been suggested to be important in human breast epithelial cell migration and tumor metastasis [24, 25]. In neural progenitors, IQGAP1 interacts with Rac1 and Cdc42 to promote VEGF-mediated neural progenitor cell migration [26]. Based on previous evidence and the complexity required for CEC activation and migration in neovascular AMD, we addressed the hypothesis that IQGAP1 binding to Rac1GTP in CECs mediates CEC migration and transmigration of the RPE to form active CNV that would threaten vision in human neovascular AMD [2].

Materials and Methods

Animals and Ethical Statement

Iqgap1^{-/-} mice and littermate *Iqgap1*^{+/+} mice (males and females) used in this study were on a C57Bl/6J genetic background and routinely tested for *Rd1*, *Rd8* and *Gnat2* mutations. All animal procedures were approved by institutional animal care and use committee, the Institutional Biosafety Committee of the University of Utah and followed the Guide for the Care and Use of Laboratory Animals of the University of Utah and the Association for Research in Vision and Ophthalmology Statement for the Use of Animals in Ophthalmic and Vision Research. Inhalation of isoflurane was used for animal anesthesia, and cervical dislocation was performed for euthanasia under anesthesia.

Laser-induced CNV model

Anesthetized 6-week-old mice were treated with laser to induce CNV. As described previously [27], eyes were first dilated with 1% tropicamide ophthalmic solution with 0.5% proparacaine hydrochloride Ophthalmic solution for pain control (California Pet Pharmacy, Hayward, CA). After dilation, mice were treated with laser using the Phoenix Image-Guided Laser System 94 (Phoenix Micron IV, Pleasanton, CA) at settings of ~460 mW intensity and 100 ms duration. Generation of cavitation bubbles, indicating disruption of Bruch's membrane, was considered successful treatment. Each eye had 4 laser spots, and each spot was located approximately 2 disc diameters from the optic nerve. Seven days after laser, mice were euthanized, and eyes were collected for the analysis of CNV volume or proteins.

Preparation of RPE/choroid flat mounts and Quantification of CNV volume

After enucleation, eyes were first fixed in 4% paraformaldehyde (Electron Microscopy Sciences, Hatfield, PA) for 1 hour. After removing the cornea, lens, vitreous and retina, the posterior eyecups consisting of the RPE/choroid/sclera were fixed in 4% paraformaldehyde for 1 additional hour. After 30 minutes blocking in phosphate-buffered saline containing 1% bovine serum albumin (BSA) and 0.5% TritonX-100 at room temperature, the posterior eyecups were stained with AlexaFluor 568-conjugated Isolectin B4 (1:500, Invitrogen, Carlsbad, CA) overnight at 4°C to label invading CECs and vessels. After staining, the eyecups were flattened by cutting radial incisions and flatmounted onto a microscope slide with vectashield mounting medium (Vector Laboratories, Burlingame, CA). Confocal z-

stack images of each lesion at 568 nm were acquired using a 20X objective using Confocal Laser Scanning Microscope (Olympus Corporation, Japan). Images were imported into IMARIS (the Oxford Instruments, Switzerland), and lesion volume was measured using the Surfaces Module (Version 9.1.2, Bitplane, Santa Barbara, California, USA). Laser spots with obvious hemorrhage or bridging CNV were excluded.

Immunostaining in Human paraffin-embedded ocular section and mouse Retinal Cryosections

IQGAP1 immunostaining was performed in paraffin embedded retinal/RPE/choroidal sections from two human donor eyes with neovascular AMD (kindly provided by Hans Grossniklaus, Emory Eye Institute, Atlanta, GA) and compared to sections lacking CNV. For staining in retinal cryosections, as described previously [12], eyes were fixed in 4% paraformaldehyde for 1 hour and then an additional hour after removing the cornea and lens. After fixation, the posterior eyecups were dehydrated in 10% sucrose for 2 hours at RT followed by 30% sucrose overnight at 4°C, and then embedded in optimal cutting temperature (OCT) (Tissue Tek, Hatfield, PA). The frozen OCT-embedded tissues were sectioned into 12 µm tissue sections using a cryotome cryostat (Thermo Fisher Scientific, Cheshire, England). After blocking in 5% normal goat serum in PBS/0.1% TritonX-100 for 1 hour at room temperature, cryosections were incubated with mouse anti-Rac1GTP (1:100; NewEast Biosciences, King of Prussia, PA) overnight at 4°C followed by 1 hour incubation with FITC-conjugated goat anti-mouse secondary antibody (1:200) (Invitrogen, Carlsbad, CA) for Rac1GTP. Isolectin B4–568 (1:500) and TO-PRO-3 (1:500, Thermo Fisher Scientific, Waltham, MA) were used to co-stain CNV lesions and nuclei, respectively. After three washes in PBS, the sections were mounted in Fluoromount-G (SouthernBiotech, Birmingham AL). Images were captured using a confocal microscope (FV1000, Olympus, Japan).

Choroidal Endothelial Cell Culture, siRNA or Plasmid DNA Transfection and Treatment

Human CECs were isolated from eyes of 3 different human donors obtained from Utah Lions Eye Bank (Salt Lake City, UT). As described previously [28], CD31 coated Dynabeads were used to pull down CECs. Cells at passages 2–5 were grown in Endothelial Growth Medium-2 (EGM-2; Lonza, Walkersville, MD) with 5% fetal bovine serum (FBS). Confirmation of phenotype of CECs was determined by >95% positive labeling with endothelial cell markers, ve-cadherin, von Willebrand factor, and CD31. Experimental outcomes were replicated using CECs from three different donors.

To knockdown endogenous IQGAP1 or introduce exogenous IQGAP1, CECs at 70–80% confluence were transfected with siRNA targeting human *Iqgap1* gene (Applied Biosystems, Foster City, CA) or plasmids expressing GFP-tagged full length IQGAP1 (pEGFP-IQ-WT) or IQGAP1 that has 24 amino acids deleted from the GRD (pEGFP-IQ-MK24) [29], rendering it unable to bind Rac1, using lipofectamine 3000 (Invitrogen). A silencer selective negative control siRNA (Applied Biosystems) was used as a control for IQGAP1 knockdown. For treatments, CECs were first starved in Endothelial Basal Medium-2 (EBM-2; Lonza) for 3 hours and then treated with recombinant human VEGF (50 ng/ml, R & D Systems, Minneapolis, MN) for 0, 15, 30, 60 or 120 minutes with or without

pretreatment with Saracatinib (10 nM, TOCRIS, Minneapolis, MN), a specific Src family kinase inhibitor, for 30 minutes. Appropriate controls for VEGF and/or Saracatinib were used and volumes/well were consistent in each experiment. After treatments, CECs were collected for different assays.

Immunoprecipitation and Western Blots

CECs were lysed in radioimmunoprecipitation assay (RIPA) buffer containing protease inhibitors (Roche Diagnostics, Indianapolis, IN) and phosphatase inhibitors (Thermo Scientific, Rockford, IL). Cell lysates were processed by immunoprecipitation (IP) with antibodies to VEGFR2, or Rac1GTP with 10 μ l of Dynabeads protein G (Invitrogen, Carlsbad, CA) by gently rocking at 4°C overnight. The antibody/protein/agarose complex was washed three times with RIPA buffer and re-suspended in 2X sample buffer. The protein complex bound to VEGFR2 (Cell signaling Technology Inc., Danvers, MA) or GTP-Rac1 (NewEast Bioscience, King of Prussia, PA) was separated by NuPAGE 4% to 12% Bis-Tris Gels (Invitrogen, Carlsbad, CA) and transferred to a PVDF membrane, incubated with antibodies to VEGFR2, p-Tyr, p-Src (Cell signaling Technology Inc.), IQGAP1 (BD Transduction Laboratories, Franklin Lakes, NJ), or total Rac1 (BD Transduction Laboratories, Franklin Lakes, NJ) overnight at 4°C. Where indicated, membranes were re-probed with β -actin as a loading control.

By co-IP, phosphorylated VEGFR2 (p-VEGFR2) was measured in RPE/choroid tissue lysate following the same protocol described above. Briefly, the total VEGFR2 was pulled down by anti-VEGFR2 antibody and the amount of p-VEGFR2 in the IP product was measured by Western blots using anti-phospho-Tyr antibody (BD Transduction Laboratories). In the same tissue lysate, VEGF, total VEGFR2, p-Src and total Src, IQGAP1, IQGAP2 (abcam, Cambridge, MA) and IQGAP3 (abcam) were also measured by Western blots using antibodies to VEGF (Santa Cruz Biotechnology, Dallas, Texas) VEGFR2, p-Src and total Src (Cell signaling Technology).

Densitometry analysis was done on exposed films with the use of the software UN-SCAN-IT version 7.1 (Silk Scientific, Orem, UT).

CEC Migration and Tube Formation Assays

Migration assays were performed in 24-well plates coated with Matrigel mixed with recombinant human VEGF (50 ng/ml, R & D Systems) or control PBS. Growth factor reduced Matrigel (Corning, Tewksbury, MA) was first diluted at 1:1 with serum free endothelial basal media (EBM-2; Lonza). Twenty-four-well plates were coated with 100 μ l of Matrigel mixed either with VEGF or PBS for 3 hours at room temperature. 500 μ l of EBM-2 was added to each well of a 24-well plate followed by a 6.5 mm diameter Transwell insert (8 μ m pores; Corning, NY). CECs stained with Vybrant DiO (Invitrogen, Carlsbad, CA) for 30 minutes at 37°C were seeded into the inserts at 50,000 cells per 100 μ l of serum free EBM-2 media. The plates were allowed to incubate overnight at 37 °C, 5% CO₂. The migrated CECs were imaged with an Olympus CK40 microscope and Olympus DP71 camera (Olympus Corporation, Japan).

For the tube formation assay, growth factor-reduced Matrigel (Corning, New York) thawed overnight was plated on 48-well plates and incubated for 30 minutes at 37°C to solidify. CECs (P3–P4) labeled with Vybrant solution (1:200, Thermofisher Scientific) in EBM-2 were seeded on top of Matrigel at 40,000/well. After 12 hours of incubation, tubes were imaged using an inverted scanning laser confocal (Olympus) at x4 magnification. Images were imported into FIJI software and the number of tube cavitations were quantified.

To determine the effects of Rac1 and Src on tube formation, CECs were treated with vehicle control, Src inhibitor (10 nM), Rac1 inhibitor (50 µM, EMD Millipore, Burlington, MA), or a combination of Src inhibitor and Rac1 inhibitor in addition to incubation with VEGF (25 ng/mL) or PBS.

To determine the effects of *Iqgap1* on tube formation, CECs were transduced with an adenovirus containing control or *IQGAP1*shRNA (kindly provided by Dr. William A Muller, Northwestern University, Chicago IL) [30] for 36 hours prior to staining, seeding, and treating with VEGF or PBS.

Statistical Analysis

A mixed effects linear regression model was used to statistically analyze CNV lesions using STATA-14 software (StataCorp LLC, College Station, TX). The model included both fixed and random effects to account for biological variation between litters by comparing experimental to control groups inside the same litter. Only one eye from each animal was used for analysis of CNV lesions, and the fellow eye was used for protein analysis. A two-tailed t-test was used for protein analysis and *in vitro* studies. Results were displayed as Mean ± SEM or SD (cell culture experiments). A minimum *P* value of <0.05 was considered statistically significant. For animal studies, at least 40 CNV spots from at least 10 animals were analyzed based on power analyses. For immunolabeled cryosections, 3–4 sections at 60 µm intervals were taken from one eye, and a total of 3 eyes from different animals were included in each group. For protein analyses, each treatment included at least 6 different animals from 3 litters. For *in vitro* studies, each experimental condition included an n=3–6 from at least two independent experiments.

Results

IQGAP1 is localized in human and experimental CNV.

The IQGAP family consists of three multi-domain scaffolding proteins, IQGAP1, IQGAP2 and IQGAP3 (Fig. 1). IQGAP1 is the most studied of the three IQGAP proteins, particularly in regulating angiogenesis [31, 32]. To address the hypothesis that IQGAP1 regulates CNV formation, we first determined if IQGAP1 was present in CNV. As shown in Figure 2, IQGAP1 staining localized strongly to human CNV but minimally in regions outside CNV, mainly to the retinal ganglion cell layer (Fig. 2a). IQGAP1 colocalization with lectin in retinal/RPE/choroidal cryosections from laser-treated wild type C57Bl6J mice was demonstrated in lectin-stained CNV and endothelial cells (Fig. 2b).

IQGAP1 knockout mice have reduced CNV.

As shown in Fig. 2, IQGAP1 localized in human and experimental CNV. We, therefore, predicted that IQGAP1 would be necessary for CNV. To test this hypothesis, we first confirmed knockout of IQGAP1 by measuring RPE/choroid for IQGAP1 protein in *Iqgap1*^{-/-} mice and compared them to control *Iqgap1*^{+/+} mice (Fig. 3a) and also measured possible compensation from IQGAP2 (Fig. 3b and c) or IQGAP3 (Fig. 3d and e). Having confirmed knockout of IQGAP1 in choroid without compensatory increases in IQGAP2 and IQGAP3, we then treated six-week old *Iqgap1*^{-/-} and littermate *Iqgap1*^{+/+} mice with laser, and analyzed the RPE/choroid flat mounts for lectin-stained CNV 7 days later. CNV volumes quantified using Imaris software were significantly lower in *Iqgap1*^{-/-} than littermate *Iqgap1*^{+/+} mice (Fig. 3f and g), providing evidence that IQGAP1 was involved in experimental CNV. There was no significant difference in CNV volumes between male and female *Iqgap1*^{-/-} (p=0.569) and *Iqgap1*^{+/+} (p=0.46) mice (data not shown).

Reduced CNV in *Iqgap1*^{-/-} mice is associated with decreased activation of VEGF receptor 2 (VEGFR2).

VEGF signaling through its angiogenic receptor, VEGFR2, is implicated in the pathogenesis of AMD [33, 34], and we and others previously reported that inhibition of VEGF with an intravitreal neutralizing anti-VEGF antibody significantly inhibited laser-induced CNV [12, 35–37]. We, therefore, determined if reduced CNV in *Iqgap1*^{-/-} mice involved VEGF or VEGF signaling. VEGF, total VEGFR2 and phosphorylation of VEGFR2 (p-VEGFR2) were measured in RPE/choroids from mice 7 days after laser treatment. As shown in Fig. 4, compared to *Iqgap1*^{+/+} mice, VEGF protein measured by western blots was significantly increased in *Iqgap1*^{-/-} mice (Fig. 4a and b). In contrast, activation of VEGFR2 determined by the ratio of p-VEGFR2 to total VEGFR2 was significantly decreased in the same tissue lysates (Fig. 4c and d). These findings suggest that IQGAP1 interacted with VEGFR2 signaling in experimental CNV but that VEGF expression was increased when IQGAP1 was broadly knocked out.

We previously reported that Rac1 activation was required for VEGF-mediated CEC migration [11, 28]. We, therefore, determined if reduced CNV in *Iqgap1*^{-/-} mice was related to decreased Rac1 activation. Rac1GTP immunostaining was performed in whole retinal cryosections. As shown in Fig. 4e and f, Rac1GTP immunostaining was localized mainly to CNV, although some staining was observed in retinal blood vessels in *Iqgap1*^{+/+} mice. Fluorescent density of Rac1GTP in lectin-stained CNV was significantly lower in *Iqgap1*^{-/-} mice than in *Iqgap1*^{+/+} mice. These findings raised the question whether reduced Rac1GTP in *Iqgap1*^{-/-} mice was involved with reduced VEGFR2 signaling despite the finding of increased VEGF ligand.

Knockdown of IQGAP1 inhibits VEGF-mediated VEGFR2 and Rac1 activation in CECs.

The results in Fig. 3 and 4 support the hypothesis that IQGAP1 is involved in CNV. IQGAP1 has been shown to associate with VEGFR2 [31]. To address the question of whether an interaction between IQGAP1 and VEGFR2 was involved in Rac1GTP-induced activation of CECs, we first determined if IQGAP1 interacted with VEGFR2 and regulated VEGFR2 activation in cultured human CECs. As shown in Fig.5a, VEGF treatment promoted

interactions between IQGAP1 and VEGFR2 as measured by co-immunoprecipitation, and the interaction was abolished in cells with IQGAP1 knockdown by siRNA transfection. In the same cell lysates, p-VEGFR2 measured by immunoprecipitation with anti-VEGFR2 followed by western blot with anti-p-Tyr, was induced by VEGF treatment in control siRNA transfected CECs but nearly abolished by IQGAP1 knockdown (Fig. 5b); however, total VEGFR2 was increased by IQGAP1 knockdown in the control and experimental siRNA conditions, suggesting that IQGAP1 regulated VEGFR2 activation, but not VEGFR2 expression.

Rac1GTP is known to bind directly to IQGAP1 [23, 24, 38]. We tested the prediction that VEGF-induced Rac1 activation required IQGAP1 in CECs by measuring interactions between IQGAP1 and Rac1GTP and the amount of Rac1GTP. As shown in Fig. 5c and d, VEGF treatment increased Rac1GTP/IQGAP1 interactions measured by co-immunoprecipitation and significantly increased the amount of Rac1GTP in control siRNA transfected CECs. Knockdown of IQGAP1 by siRNA prevented VEGF-mediated IQGAP1/Rac1GTP interactions and abrogated the ability of VEGF to increase Rac1GTP (Fig. 5c and d). These findings suggested that IQGAP1/Rac1GTP interactions were involved in but not necessary for all Rac1 activation. Activation of Rac1 is required for VEGF-mediated CEC migration [11, 39]. To test the hypothesis that knockdown of IQGAP1 reduced VEGF-mediated CEC migration, we silenced IQGAP1 in CECs with IQGAP1 siRNA vs. control siRNA and treated with VEGF overnight. VEGF treatment significantly increased CEC migration; however, knockdown of IQGAP1 (Supplemental Figure 1) abolished VEGF-induced CEC migration (Fig. 5e and Supplemental Figure 2a) and tube formation (Fig. 5f and Supplemental Figure 3b).

Direct Binding of Rac1GTP to GRD of IQGAP1 Sustains Rac1 Activation in CECs.

We and other investigators previously showed that the IQGAP1 GRD directly binds Rac1GTP [23, 24, 38]. To determine if Rac1GTP binding to the IQGAP1 GRD is responsible for VEGF-mediated Rac1 activation, we used IQGAP1 with deletion in the GRD (GFP-IQ-MK24) that is not able to bind Rac1GTP [24]. CECs were transfected with GFP-tagged wild type IQGAP1 (GFP-IQ-WT) or GFP-IQ-MK24 and both the interaction of Rac1GTP with IQGAP1 and the amount of Rac1GTP were measured. As shown in Fig. 6a and b, in GFP-IQ-WT transfected CECs, VEGF treatment induced Rac1GTP/IQGAP1 interactions and significantly increased the amount of Rac1GTP at 15 minutes. Induction of Rac1GTP was sustained through 120 minutes (Fig. 6b). In GFP-IQ-MK24 transfected CECs, the interaction between Rac1GTP and IQGAP1 was increased to a lesser degree after VEGF treatment, whereas Rac1GTP was significantly increased at 15 minutes following VEGF stimulation but was not sustained through 120 minutes (Fig. 6B). Together with the effects of IQGAP1 on CNV, we postulated that IQGAP1 binding Rac1GTP was necessary to sustain VEGF induced activation of Rac1GTP, which was important to cause CEC migration.

IQGAP1 regulates Rac1 activation by Src-dependent signaling.

The data in Fig. 6 provide evidence that the interaction of IQGAP1 and Rac1GTP is not required for all VEGF-mediated Rac1 activation shown at 15 minutes, but is necessary to

sustain Rac1 activation at 120 minutes, which leads to CEC migration toward a VEGF gradient over time. However, knockdown of IQGAP1 significantly decreased Rac1GTP as shown in Fig. 5. We, therefore, tested another mechanism whereby IQGAP1 affected VEGF mediated VEGFR2 activation.

Src, one of the Src family kinase family members, has been shown as an intracellular signal transducer of VEGF/VEGFR2 mediated signaling [32, 40]. Also, activated Src promotes endothelial progenitor cell migration by activating Rac1 [41]. To gain insight into the potential involvement of Src in VEGF-induced VEGFR2/IQGAP1 interactions and Rac1 activation, we first determined if Src regulated Rac1 activity in *Iqgap1*^{-/-} mice. Phosphorylated Src (p-Src) and total Src were measured by western blots in RPE/choroids from *Iqgap1*^{+/+} and *Iqgap1*^{-/-} mice 7 days after laser. As shown in Fig. 7a and b, p-Src/total Src was significantly reduced in *Iqgap1*^{-/-} mice compared to *Iqgap1*^{+/+} mice, suggesting that Src was involved in IQGAP1 mediated CNV. To determine if IQGAP1 was involved in VEGF-induced Src activation in CECs, p-Src and total Src were measured by western blots in CECs transfected with IQGAP1siRNA or controlsiRNA and treated with VEGF. In ControlsiRNA-transfected CECs, VEGF treatment at 15 minutes significantly increased Src activation determined by p-Src, which was not observed in CECs knocked down for IQGAP1 (Fig.7c and d). This suggested that IQGAP1 was necessary for VEGF-induced Src activation.

Activated VEGFR2 has been reported to recruit Src in order to activate it and this involves a physical interaction of VEGFR2 and Src via a SH2 domain in Src [40]. To test the prediction that IQGAP1 is involved in the interaction of VEGFR2 and Src and Src activation, co-immunoprecipitation (co-IP) of VEGFR2 and Src and western blot of p-Src were measured in CECs transfected with IQGAP1siRNA. As shown in Fig. 7c and d, VEGF increased co-IP of VEGFR2 and Src, and p-Src/total Src in control siRNA transfected CECs. This interaction was reduced with knockdown of IQGAP1, suggesting that IQGAP1 was necessary for Src activation induced by VEGF mediated VEGFR2 phosphorylation. Src has been shown to promote endothelial progenitor cell migration by activating Vav2 nucleotide exchange factor 2 and downstream Rac1 activation [41]. We next asked if Src activation regulates Rac1 activation in CECs. VEGF-mediated Rac1 activation was measured in CECs pretreated with the Src inhibitor, Saracatinib. As shown in Fig. 7e and f, in control CECs, p-Src and Rac1GTP were significantly induced by VEGF treatment at both 30 and 60 minutes. Pretreatment with Saracatinib efficiently blocked VEGF-induced p-Src and abrogated the increase in Rac1GTP, showing that IQGAP1-mediated Src activation induced by VEGF/VEGFR2 is also sufficient to activate Rac1GTP. To determine if Src-mediated Rac1 activation was necessary for VEGF-mediated angiogenesis, cell migration and tube formation were measured in CECs treated with Src or/and Rac1 inhibitors. As shown in Fig. 8, compared to control, treatment with either Saracatinib or Rac1 inhibitor alone significantly reduced VEGF-mediated CEC migration (Fig. 8a and Supplemental Figure 2b), suggesting that Src regulates CEC migration through activation of Rac1. Saracatinib treatment significantly reduced both PBS- and VEGF-mediated tube formation. Treatment with the Rac1 inhibitor led to a trend toward reduction in VEGF-mediated tube formation (Fig. 8b and Supplemental Figure 3b). Combined treatment with both Saracatinib and Rac1 inhibitor did not cause a further decrease in CEC migration and tube formation compared to

Saracatinib treatment alone. However, compared to Rac1 treatment alone, CECs treated with both inhibitors had a further reduction in tube formation, suggesting that Src regulates CEC tube formation not only through activation of Rac1, but also through other effectors, which will be addressed in future studies. Altogether, our results shown in Fig. 8 provide further evidence that Src-mediated Rac1 activation (Fig.7) was necessary for VEGF-mediated angiogenic effects.

Our data suggest that VEGF-induced VEGFR2 mediated sustained Rac1GTP requires binding of Rac1GTP to the GRD of IQGAP1 and may be necessary to overwhelm homeostasis and drive CEC migration. IQGAP1 is also needed in VEGF-induced Rac1GTP through the recruitment and activation of Src potentially by other mechanisms than by binding GRD.

Discussion

Neovascular AMD is a leading cause of vision loss worldwide. The introduction of anti-VEGF agents has greatly improved outcomes in visual acuity in about 40% of patients, aligning with experimental studies using neutralizing intravitreal anti-VEGF antibodies in laser-induced CNV models [12, 42–44]. One potential reason for the incomplete effect of anti-VEGF agents may be due to the complex pathophysiology of AMD, which involves the impact of many factors in addition to VEGF or that augment downstream signaling from VEGF pathways, such as through crosstalk with oxidative and inflammatory signaling factors [45, 46].

We found Rac1GTP was a common effector of multiple signaling pathways. Rac1GTP is essential for CEC transmigration of the RPE, a necessary step in the active, vision-threatening type 2 CNV of neovascular AMD [2, 47, 48]. Rac1 is also activated by TNF α , VEGF, CCL11 or NADPH-oxidase-generated ROS [27, 49, 50], and these factors or broad signaling pathways they represent have been implicated in human AMD [51–53]. We, therefore, were interested in mechanisms to regulate Rac1 activation in CECs in order to reduce CEC activation and migration, which are important in type 2 CNV. We focused on the IQGAP1 scaffold protein, which links multiple signaling cascades necessary for complex cell and biologic events [21, 23]. IQGAP1 has also been studied in angiogenesis in other endothelial beds such as by regulating VE-cadherin phosphorylation and cell-cell contacts in human umbilical vascular endothelial cells [31], or by macrophage infiltration and oxidative signaling in ischemic muscle tissue in an ischemic-induced neovascularization model [54]. However, no prior publication has addressed IQGAP1 in the choroid and outer retina and involving CECs as related to AMD. In the current study, we tested the hypothesis that IQGAP1 is involved in CEC migration and CNV and found evidence that induced Rac1GTP that directly binds IQGAP1 at the GRD domain sustains activation of Rac1, which may be necessary to drive pathologic events in CNV and neovascular AMD.

Using human samples of CNV and areas lacking CNV in donor eyes from patients with neovascular AMD, we found that IQGAP1 localized to human CNV and colocalized with lectin-labeled experimental CNV induced by laser. In the murine laser-induced CNV model, we also observed a significant reduction in CNV in *Iqgap1*^{-/-} mice compared to *Iqgap1*^{+/+}

mice. We further found decreased activation of VEGFR2 and Rac1GTP in *Iqgap1*^{-/-} mice treated with laser to induce CNV. However, we did not find that VEGF was reduced and was actually increased, suggesting compensatory increase in VEGF expression and that IQGAP1/VEGFR2 interactions were involved in CNV pathology without reducing the VEGF ligand. This effect could be beneficial to VEGF-induced survival effects on other cells and the neural retina [55–57]. Although knockdown of IQGAP1 by siRNA inhibited VEGF-stimulated VEGFR2 phosphorylation in cultured CECs, it did not reduce total VEGFR2, but rather increased it. We interpret these findings to suggest that IQGAP1 regulates VEGFR2 expression or activation such as through other mechanisms including internalization of VEGFR2 or interactions with downstream effectors. We will address these considerations in future studies.

Pathology in disease requires a number of events or feed-forward loops that overwhelm homeostatic mechanisms that restore physiologic function. In AMD, multiple factors are involved, many of which activate the GTPase, Rac1. Inflammatory mechanisms involving TNF α -induced NADPH oxidase led to a feed forward loop exacerbating Rac1 activation [45]. VEGF activates Rac1 through the GEF, Vav2 [58]. We provided evidence that knockdown of IQGAP1 inhibited VEGF-stimulated Rac1 activation in CECs; however direct binding of Rac1GTP to IQGAP1 at GRD was required for sustained activation of Rac1GTP induced by VEGF in CECs, but not for all Rac1 activation. This suggested that direct interference with Rac1GTP binding at GRD of IQGAP1 would interfere with sustained Rac1GTP signaling. These observations led us to explore other potential mechanisms whereby IQGAP1 regulates VEGF-mediated Rac1 activation. We observed a decreased p-Src in CNV from mice treated with laser to induced CNV. Additional in vitro experiments provided evidence that IQGAP1 was necessary for VEGF-mediated Rac1 activation by regulating the recruitment of Src to VEGFR2, which led to subsequent Src activation. Given the role of activated Src in activating the GEF, Vav2 [41], we predicted that inhibition of Src would reduce Rac1 activation by VEGF. Our results supported this prediction. We further show that IQGAP1 was necessary for VEGF-induced CEC migration. Our goal is not to abolish activation of Rac1GTP but rather to regulate it in CEC migration, which is induced by pathologic stimuli overwhelming homeostasis in AMD. These findings support the thinking that targeting domains in IQGAP1 may efficiently interfere with neovascular AMD without reducing VEGF or Rac1GTP, which have physiologic properties.

In conclusion, IQGAP1 in CECs interacts with VEGFR2 to mediate Src activation and subsequent Rac1 activation; IQGAP1 also binds Rac1GTP to sustain activation of Rac1, thus driving CEC transmigration toward VEGF expressed by RPE, an important event in type 2 neovascular AMD (Fig. 9). The findings from our study support the role of IQGAP1 in CNV. Targeting the interaction of IQGAP1 and Rac1GTP may restore quiescence of CECs and inhibit CEC migration, thereby preventing CNV formation in neovascular AMD without totally inhibiting VEGF or Rac1GTP related physiologic functions.

Supplementary Material

Refer to Web version on PubMed Central for supplementary material.

Acknowledgments

This work was supported by the National Institutes of Health EY014800 and an Unrestricted Grant from Research to Prevent Blindness, Inc., New York, NY, to the Department of Ophthalmology & Visual Sciences, University of Utah; and the National Institutes of Health R01EY015130 and R01EY017011 to M.E.H. D.B.S. is supported by the Intramural Research Program of the National Institutes of Health. We thank Dr. William A. Muller for providing adenovirus-IQGAP1shRNA constructs.

References

1. Zarbin MA, Current concepts in the pathogenesis of age-related macular degeneration. *Archives of Ophthalmology*, 2004 122(4): p. 598–614. [PubMed: 15078679]
2. Hartnett ME and Elsner AE, Characteristics of exudative age-related macular degeneration determined in vivo with confocal and indirect infrared imaging. *Ophthalmology*, 1996 103(1): p. 58–71. [PubMed: 8628562]
3. Freund KB, Zweifel SA, and Engelbert M, Do we need a new classification for choroidal neovascularization in age-related macular degeneration? *Retina*, 2010 30(9): p. 1333–49. [PubMed: 20924258]
4. Hartnett ME and Elsner AE, Characteristics of exudative age-related macular degeneration determined in vivo with confocal and indirect infrared imaging. *Ophthalmology*, 1996 103: p. 58–71. [PubMed: 8628562]
5. Daniel E, et al., Five-Year Follow-up of Nonfibrotic Scars in the Comparison of Age-Related Macular Degeneration Treatments Trials. *Ophthalmology*, 2019 126(5): p. 743–751. [PubMed: 30476517]
6. Pershing S, et al., Use of Bevacizumab and Ranibizumab for Wet Age-Related Macular Degeneration: Influence of CATT Results and Introduction of Aflibercept. *Am J Ophthalmol*, 2019 207: p. 385–394. [PubMed: 31100217]
7. Jaffe GJ, et al., Macular Morphology and Visual Acuity in Year Five of the Comparison of Age-related Macular Degeneration Treatments Trials. *Ophthalmology*, 2019 126(2): p. 252–260. [PubMed: 30189282]
8. Engers R, et al., Rac affects invasion of human renal cell carcinomas by up-regulating tissue inhibitor of metalloproteinases (TIMP)-1 and TIMP-2 expression. *Journal of Biological Chemistry*, 2001 276(45): p. 41889–41897. [PubMed: 11551917]
9. Ridley AJ, et al., Cell migration: integrating signals from front to back. *Science*, 2003 302(5651): p. 1704–1709. [PubMed: 14657486]
10. Burridge K, Crosstalk between Rac and Rho. *Science*, 1999 283: p. 2028–2029. [PubMed: 10206910]
11. Peterson LJ, et al., Heterotypic RPE-choroidal endothelial cell contact increases choroidal endothelial cell transmigration via PI 3-kinase and Rac1. *Experimental Eye Research*, 2007 In Press.
12. Wang H, et al., Retinal pigment epithelial cell expression of active Rap 1a by scAAV2 inhibits choroidal neovascularization. *Mol Ther Methods Clin Dev*, 2016 3: p. 16056. [PubMed: 27606349]
13. Wang H, et al., TNF-alpha mediates choroidal neovascularization by upregulating VEGF expression in RPE through ROS-dependent beta-catenin activation. *Mol Vis*, 2016 22: p. 116–28. [PubMed: 26900328]
14. Monaghan-Benson E and Burridge K, The regulation of VEGF-induced microvascular permeability requires Rac and ROS. *Journal of Biological Chemistry*, 2009: p. M109.
15. Wittchen ES, et al., Rap1 GTPase inhibits leukocyte transmigration by promoting endothelial barrier function. *Journal of Biological Chemistry*, 2005 280: p. 11675–11682. [PubMed: 15661741]
16. Burridge K and Wennerberg K, Rho and Rac take center stage. *Cell*, 2004 116(2): p. 167–179. [PubMed: 14744429]

17. Panday A, et al., NADPH oxidases: an overview from structure to innate immunity-associated pathologies. *Cell Mol Immunol*, 2015 12(1): p. 5–23. [PubMed: 25263488]
18. Acevedo A and Gonzalez-Billault C, Crosstalk between Rac1-mediated actin regulation and ROS production. *Free Radic Biol Med*, 2018 116: p. 101–113. [PubMed: 29330095]
19. Bid HK, et al., RAC1: an emerging therapeutic option for targeting cancer angiogenesis and metastasis. *Mol Cancer Ther*, 2013 12(10): p. 1925–34. [PubMed: 24072884]
20. Bergers G and Benjamin LE, Tumorigenesis and the angiogenic switch. *Nat Rev Cancer*, 2003 3(6): p. 401–10. [PubMed: 12778130]
21. Hedman AC, Smith JM, and Sacks DB, The biology of IQGAP proteins: beyond the cytoskeleton. *EMBO Rep*, 2015 16(4): p. 427–46. [PubMed: 25722290]
22. White CD, Erdemir HH, and Sacks DB, IQGAP1 and its binding proteins control diverse biological functions. *Cell Signal*, 2012 24(4): p. 826–34. [PubMed: 22182509]
23. Mataraza JM, et al., IQGAP1 promotes cell motility and invasion. *J Biol Chem*, 2003 278(42): p. 41237–45. [PubMed: 12900413]
24. Mataraza JM, et al., Multiple proteins mediate IQGAP1-stimulated cell migration. *Cell Signal*, 2007 19(9): p. 1857–65. [PubMed: 17544257]
25. Jadeski L, et al., IQGAP1 stimulates proliferation and enhances tumorigenesis of human breast epithelial cells. *J Biol Chem*, 2008 283(2): p. 1008–17. [PubMed: 17981797]
26. Balenci L, et al., IQGAP1 regulates adult neural progenitors in vivo and vascular endothelial growth factor-triggered neural progenitor migration in vitro. *J Neurosci*, 2007 27(17): p. 4716–24. [PubMed: 17460084]
27. Wang H, et al., Rap1 GTPase Inhibits Tumor Necrosis Factor-alpha-Induced Choroidal Endothelial Migration via NADPH Oxidase- and NF-kappaB-Dependent Activation of Rac1. *Am J Pathol*, 2015 185(12): p. 3316–25. [PubMed: 26476350]
28. Geisen P, McColm JR, and Hartnett ME, Choroidal endothelial cells transmigrate across the retinal pigment epithelium but do not proliferate in response to soluble vascular endothelial growth factor. *Experimental Eye Research*, 2006 82: p. 608–619. [PubMed: 16259980]
29. Mataraza JM, et al., Identification and characterization of the Cdc42-binding site of IQGAP1. *Biochem Biophys Res Commun*, 2003 305(2): p. 315–21. [PubMed: 12745076]
30. Sullivan DP, et al., Endothelial IQGAP1 regulates leukocyte transmigration by directing the LBRC to the site of diapedesis. *The Journal of experimental medicine*, 2019 216(11): p. 2582–2601. [PubMed: 31395618]
31. Yamaoka-Tojo M, et al., IQGAP1 Mediates VE-Cadherin-Based Cell-Cell Contacts and VEGF Signaling at Adherence Junctions Linked to Angiogenesis. *Arteriosclerosis, Thrombosis, and Vascular Biology*, 2006 26(9): p. 1991–1997.
32. Meyer RD, Sacks DB, and Rahimi N, IQGAP1-dependent signaling pathway regulates endothelial cell proliferation and angiogenesis. *PLoS One*, 2008 3(12): p. e3848. [PubMed: 19050761]
33. Huang H, Shen J, and Vinore SA, Blockade of VEGFR1 and 2 suppresses pathological angiogenesis and vascular leakage in the eye. *PLoS One*, 2011 6(6): p. e21411. [PubMed: 21731737]
34. Cruz-Gonzalez F, et al., Predictive value of VEGF A and VEGFR2 polymorphisms in the response to intravitreal ranibizumab treatment for wet AMD. *Graefes Arch Clin Exp Ophthalmol*, 2014 52(3): p. 469–75. [PubMed: 24522370]
35. Askou AL, et al., Suppression of Choroidal Neovascularization by AAV-Based Dual-Acting Antiangiogenic Gene Therapy. *Molecular therapy. Nucleic acids*, 2019 16: p. 38–50. [PubMed: 30825671]
36. Lukason M, et al., Inhibition of choroidal neovascularization in a nonhuman primate model by intravitreal administration of an AAV2 vector expressing a novel anti-VEGF molecule. *Mol Ther*, 2011 19(2): p. 260–5. [PubMed: 20978476]
37. Martin DF, Evolution of Intravitreal Therapy for Retinal Diseases - From CMV to CNV: The LXXIV Edward Jackson Memorial Lecture. *Am J Ophthalmol*, 2018.
38. Owen D, et al., The IQGAP1-Rac1 and IQGAP1-Cdc42 interactions: interfaces differ between the complexes. *J Biol Chem*, 2008 283(3): p. 1692–704. [PubMed: 17984089]

39. Wang H, et al., The Role of RPE Cell-Associated VEGF189 in Choroidal Endothelial Cell Transmigration across the RPE. *Investigative Ophthalmology & Visual Science*, 2011 52(1): p. 570–578. [PubMed: 20811045]
40. Mezquita B, et al., Unlocking Doors without Keys: Activation of Src by Truncated C-terminal Intracellular Receptor Tyrosine Kinases Lacking Tyrosine Kinase Activity. *Cells*, 2014 3(1): p. 92–111. [PubMed: 24709904]
41. Li Z, et al., Mesenchymal stem cells promote endothelial progenitor cell migration, vascularization, and bone repair in tissue-engineered constructs via activating CXCR2-Src-PKL/Vav2-Rac1. *Faseb j*, 2018 32(4): p. 2197–2211. [PubMed: 29229683]
42. Joussen AM and Bornfeld N, The treatment of wet age-related macular degeneration. *Dtsch Arztebl Int*, 2009 106(18): p. 312–7. [PubMed: 19547647]
43. Haller JA, Current anti-vascular endothelial growth factor dosing regimens: benefits and burden. *Ophthalmology*, 2013 120(5 Suppl): p. S3–7. [PubMed: 23642784]
44. Rofagha S, et al., Seven-Year Outcomes in Ranibizumab-Treated Patients in ANCHOR, MARINA, and HORIZON: A Multicenter Cohort Study (SEVEN-UP). *Ophthalmology*, 2013.
45. Wang H and Hartnett ME, Regulation of signaling events involved in the pathophysiology of neovascular AMD. *Mol Vis*, 2016 22: p. 189–202. [PubMed: 27013848]
46. Handa JT, et al., A systems biology approach towards understanding and treating non-neovascular age-related macular degeneration. *Nat Commun*, 2019 10(1): p. 3347. [PubMed: 31350409]
47. Farecki ML, et al., Characteristics of type 1 and 2 CNV in exudative AMD in OCT-Angiography. *Graefes Arch Clin Exp Ophthalmol*, 2017 255(5): p. 913–921. [PubMed: 28233061]
48. Grunwald JE, et al., Photographic assessment of baseline fundus morphologic features in the Comparison of Age-Related Macular Degeneration Treatments Trials. *Ophthalmology*, 2012 119(8): p. 1634–41. [PubMed: 22512984]
49. Monaghan-Benson E, et al., The Role of Vascular Endothelial Growth Factor-Induced Activation of NADPH Oxidase in Choroidal Endothelial Cells and Choroidal Neovascularization. *The American Journal of Pathology*, 2010 177(4): p. 2091–2102. [PubMed: 20802176]
50. Wang H, et al., Retinal Inhibition of CCR3 Induces Retinal Cell Death in a Murine Model of Choroidal Neovascularization. *PLoS One*, 2016 11(6): p. e0157748. [PubMed: 27309355]
51. Takeda A, et al., CCR3 is a target for age-related macular degeneration diagnosis and therapy. *Nature*, 2009 460(7252): p. 225–230. [PubMed: 19525930]
52. Wang H, et al., Upregulation of CCR3 by Age-Related Stresses Promotes Choroidal Endothelial Cell Migration via VEGF-Dependent and -Independent Signaling. *Investigative Ophthalmology & Visual Science*, 2011 52(11): p. 8271–8277. [PubMed: 21917937]
53. Churchill AJ, et al., VEGF polymorphisms are associated with neovascular age-related macular degeneration. *Human Molecular Genetics*, 2006 15(19): p. 2955–2961. [PubMed: 16940309]
54. Urao N, et al., Role of nox2-based NADPH oxidase in bone marrow and progenitor cell function involved in neovascularization induced by hindlimb ischemia. *Circ Res*, 2008 103(2): p. 212–20. [PubMed: 18583711]
55. Becker S, et al., Targeted Knockdown of Overexpressed VEGFA or VEGF164 in Muller cells maintains retinal function by triggering different signaling mechanisms. *Sci Rep*, 2018 8(1): p. 2003. [PubMed: 29386650]
56. Saint-Geniez M, et al., Endogenous VEGF is required for visual function: evidence for a survival role on muller cells and photoreceptors. *PLoS One*, 2008 3(11): p. e3554. [PubMed: 18978936]
57. D'Amore PA and Smith SR, Growth factor effects on cells of the vascular wall: a survey. *Growth Factors*, 1993 8(1): p. 61–75. [PubMed: 7680568]
58. Abe K, et al., Vav2 Is an activator of Cdc42, Rac1, and RhoA. *Journal of Biological Chemistry*, 2000 275(14): p. 10141–10149. [PubMed: 10744696]

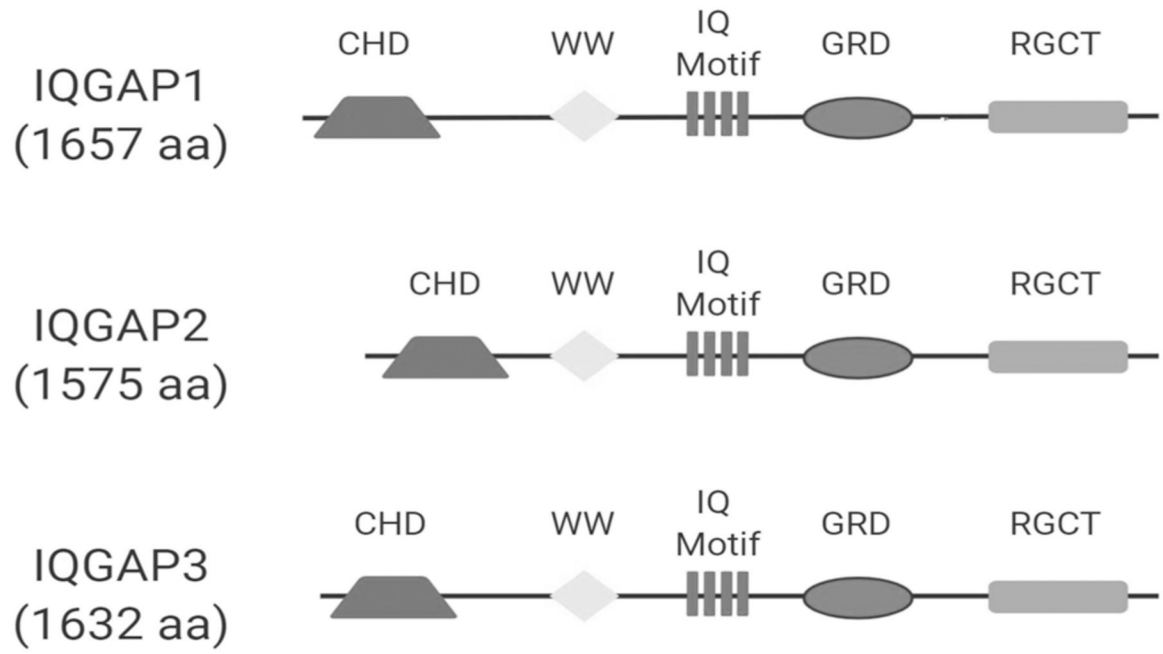


Fig. 1. Isoforms of IQGAP family proteins: IQGAP1, IQGAP2 and IQGAP3.
All the isoforms contain a GRD domain.

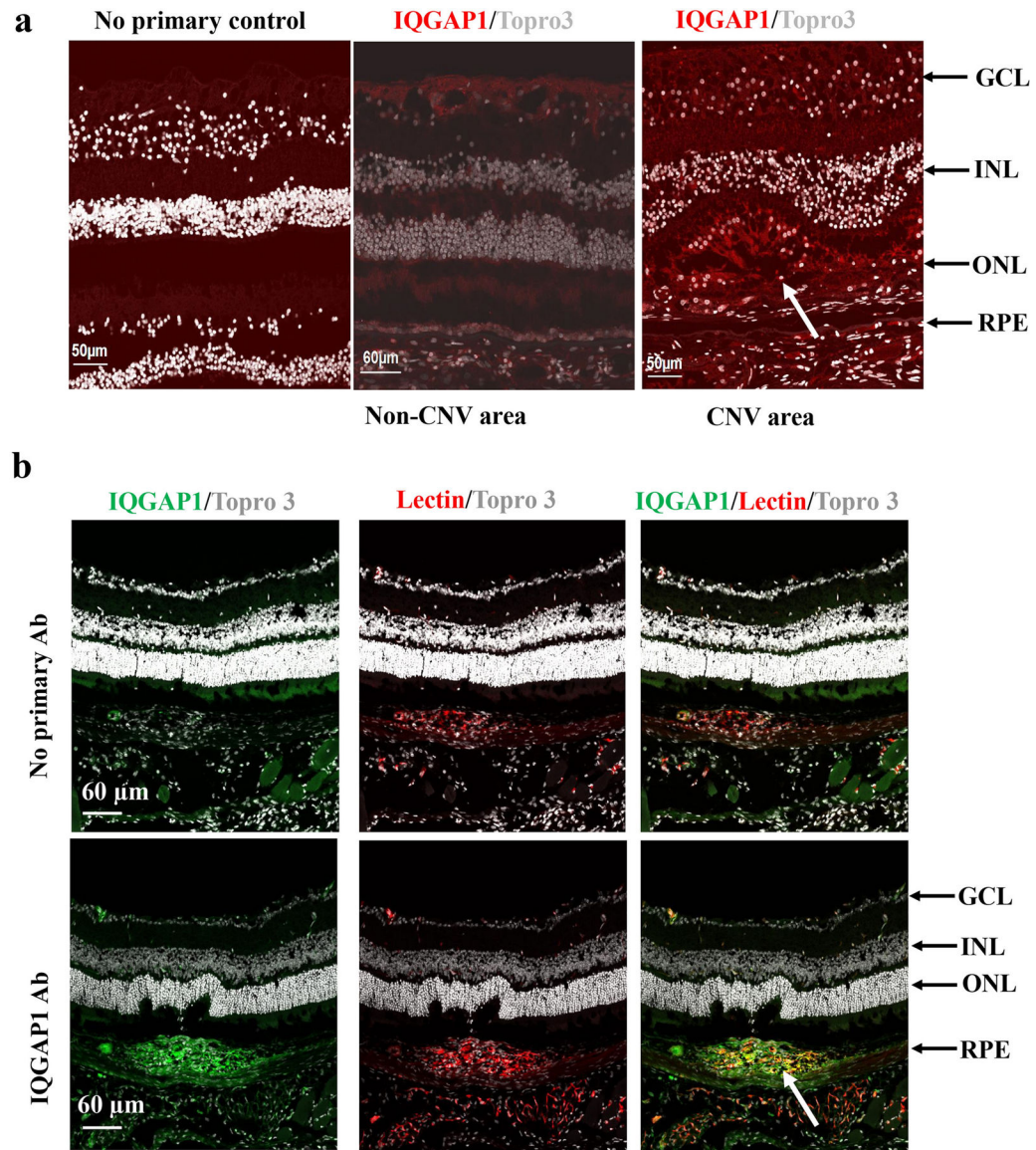


Fig. 2. IQGAP1 is located at CNV lesions.

(a) Immunostaining of IQGAP1 in retinal sections of human donor eyes with AMD (Red: IQGAP1; Gray: Topro 3 to stain nuclei); (b) immunostaining of IQGAP1 and isolectin in retinal cryosections of wild type mice treated with laser (Green: IQGAP1; Red: isolectin; Gray: Topro3 to stain nuclei; GCL, ganglion cell layer; INL, inner nuclear layer; ONL, outer nuclear layer; RPE, retinal pigment epithelium; the white arrows point to type 2 CNV).

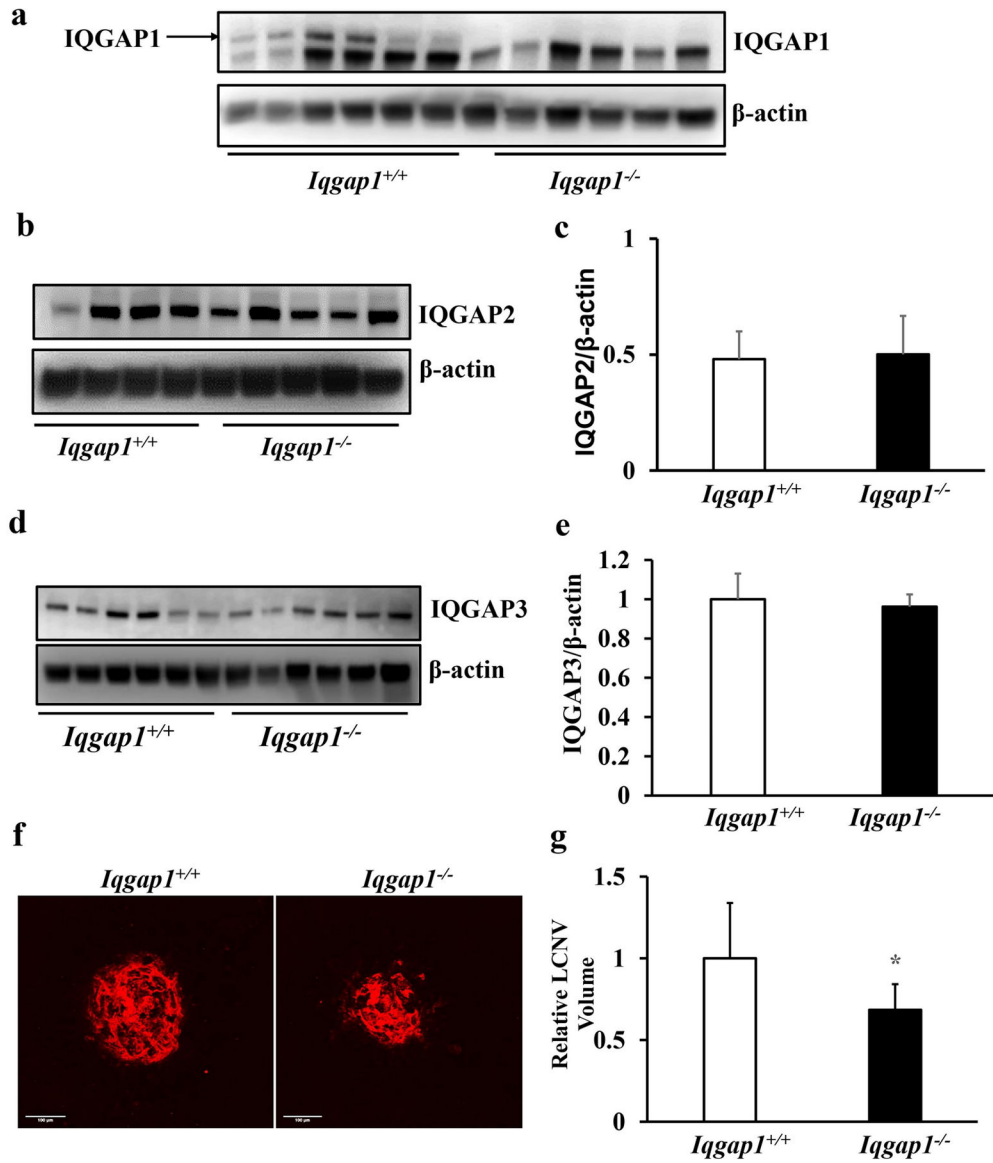


Fig. 3. *Iqgap1*^{-/-} mice show reduced CNV in a laser-induced CNV model. Western blots of (a) IQGAP1, (b-c) IQGAP2, and (d-e) IQGAP3 in RPE/choroids of *Iqgap1*^{+/+} and *Iqgap1*^{-/-} mice 7 days post laser treatment (b and d, representative gel images, and c and e, quantification of densitometry); (f) Representative images of RPE/choroid flat mounts and (g) quantification of CNV lesion (*p<0.05 vs. *Iqgap1*^{+/+} mice, n=52 spots from 14 mice) in *Iqgap1*^{+/+} and *Iqgap1*^{-/-} mice 7 days post laser treatment.

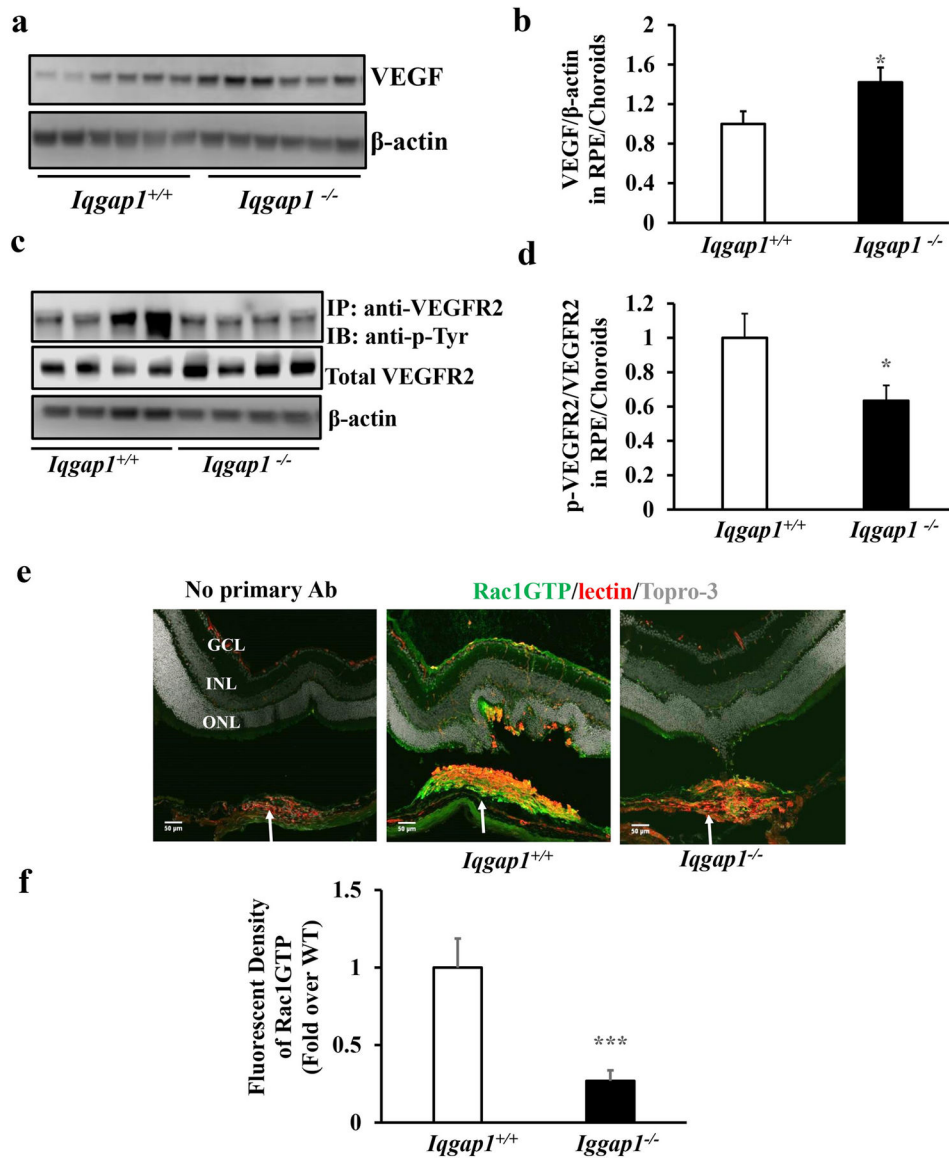


Fig. 4. *Iqgap1*^{-/-} mice show increased VEGF and decreased VEGFR2 and Rac1 activation in a laser-induced CNV model.

(a and b) western blots of VEGF and β -actin, (c and d) co-immunoprecipitation of VEGFR2 (p-VEGFR2) and western blots of p-Tyr, total VEGFR2 and β -actin in RPE/choroids, and (e and f) immunostaining of GTP-Rac1, isolectin and Topro 3 in retinal cryosections (Green: GTP-Rac1; Red: isolectin; Gray: Topro 3; GCL, ganglion cell layer; INL, inner nuclear layer; ONL, outer nuclear layer) of *Iqgap1*^{+/+} and *Iqgap1*^{-/-} mice 7 days post laser treatment (a, c and e, representative gel images and b, d and f, quantification of densitometry and fluorescence density of GTP-Rac1 at isolectin stained CNV lesions; * $p < 0.05$, *** $p < 0.001$ vs. *Iqgap1*^{+/+} mice; $n = 6-8$; white arrows point to type 2 CNV).

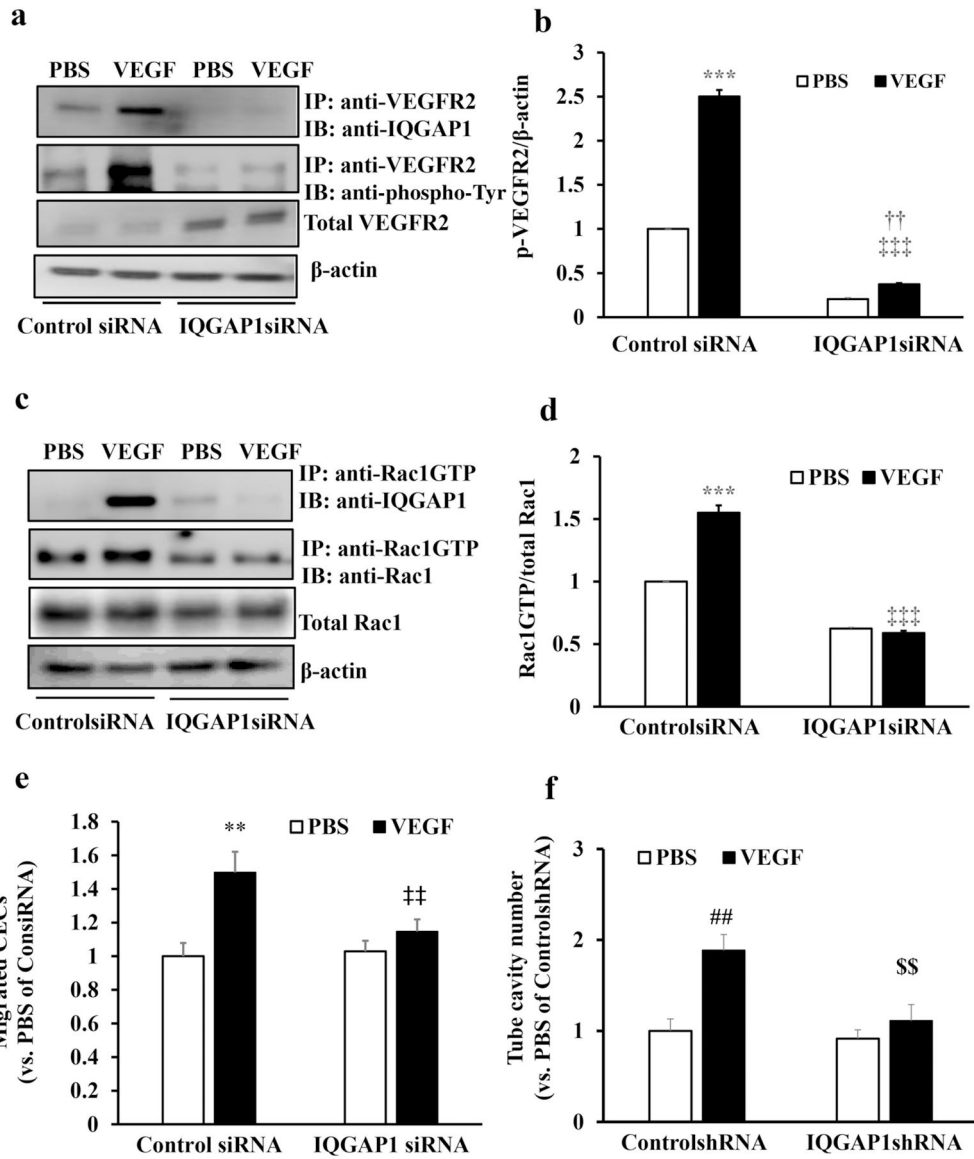


Fig. 5. IQGAP1 regulates VEGF-mediated VEGFR2 activation and Rac1 activation. (a–b) co-immunoprecipitation of VEGFR2 and IQGAP1 and phosphorylated VEGFR2 (p-VEGFR2) and western blots of total VEGFR2, IQGAP1, and β -actin in CECs transfected with IQGAP1 siRNA or control siRNA and treated with VEGF for 15 mins; (c–d) co-immunoprecipitation of GTP-Rac1 and IQGAP1, and GTP-Rac1 determined by immunoprecipitation with anti-GTP-Rac1 and western blot of total Rac1 in CECs transfected with IQGAP1 siRNA or control siRNA and treated with VEGF for 30 mins; (e) cell migration toward VEGF of CECs transfected with IQGAP1 siRNA or control siRNA and (f) tube formation induced by VEGF of CECs transfected with adenovirus-delivered IQGAP1shRNA or controlshRNA (** $p < 0.01$, *** $p < 0.001$ vs. PBS of controlsiRNA, †† $p < 0.01$ vs. PBS of IQGAP1siRNA, † $p < 0.05$, ††† $p < 0.001$ vs. VEGF of ControlsiRNA; ## $p < 0.01$ vs. PBS of ControlshRNA and \$\$ $p < 0.01$ vs. VEGF of ControlshRNA; $n = 3-6$).

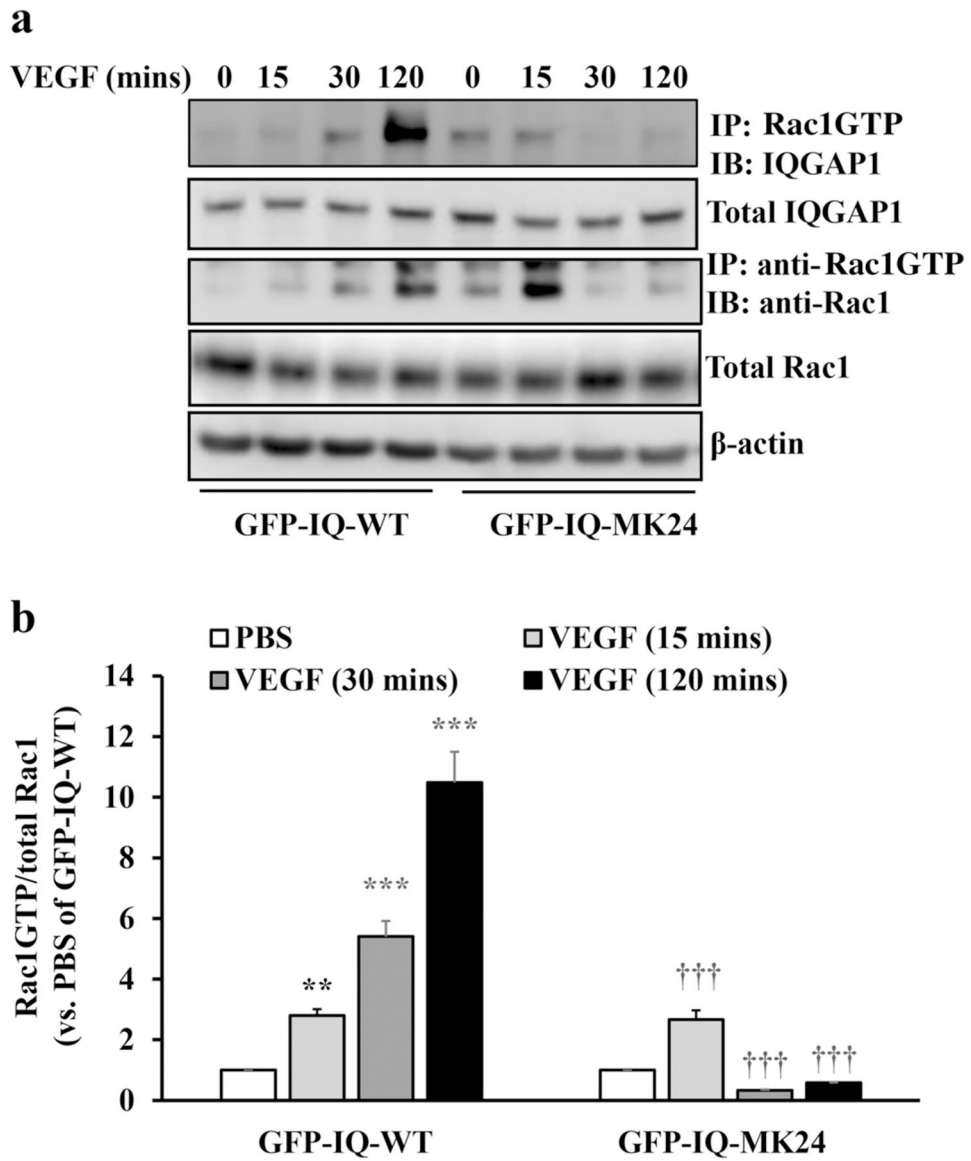


Fig. 6. Direct binding of Rac1GTP to GRD of IQGAP sustains Rac1 activation. Co-immunoprecipitation of GTP-Rac1 and IQGAP1, and GTP-Rac1 determined by immunoprecipitation with anti-GTP-Rac1 and western blot of total Rac1 in CECS transfected with plasmid DNAs expressing full length IQGAP1 (GFP-IQ-WT) or mutant GRD (GFP-IQ-MK24) and treated with VEGF for for 15, 30, 120 mins or PBS control (a, representative gel images, and b, quantification of densitometry; ** $p < 0.01$, *** $p < 0.001$ vs. PBS of GFP-IQ-WT, ††† $p < 0.001$ vs. PBS of GFP-IQ-MK24; $n = 3$).

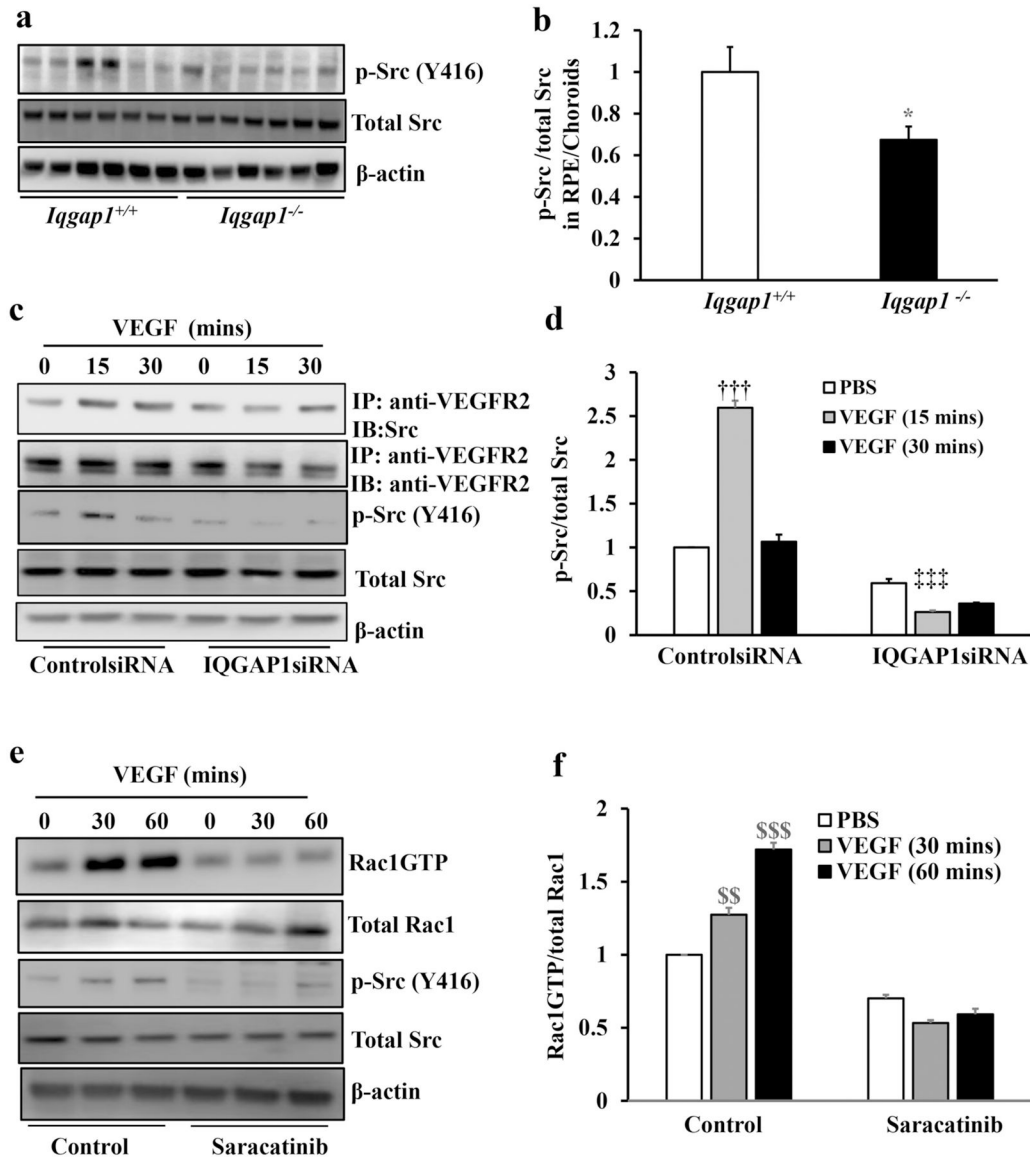


Fig. 7. IQGAP1 regulates Rac1 activation by mediating Src activation.

(a and b) Western blots of phosphorylated Src (p-Src), total Src and β -actin in RPE/choroids of *Iqgap1*^{+/+} and *Iqgap1*^{-/-} mice 7 days post laser treatment (*p < 0.05 vs. *Iqgap1*^{+/+} mice; n = 6–8; a, representative gel images and b, quantification of densitometry); (c–d) western blots of p-Src, total Src, IQGAP1 and β -actin and co-immunoprecipitation of VEGFR2 and Src, and western blots of total VEGFR2, p-Src total Src and β -actin in CECs transfected with IQGAP1 siRNA or control siRNA and treated with VEGF for 15 or 30 mins; and (e–f) activation of Rac1 determined by immunoprecipitation of anti-GTP-Rac1 and western blot of total Rac1, and western blots of total Rac1, p-Src, total Src and β -actin in CECs pretreated with Src inhibitor, Saracatinib (10 nM), for 30 mins followed by VEGF treatment for 30 or 60 mins (††p < 0.01 vs. PBS of Control siRNA, †††p < 0.001 vs. PBS of IQGAP1 siRNA, \$\$\$p < 0.01, \$\$\$\$p < 0.001 vs. PBS of Control, n = 3; c and e, representative gel images, and d and f, quantification of densitometry).

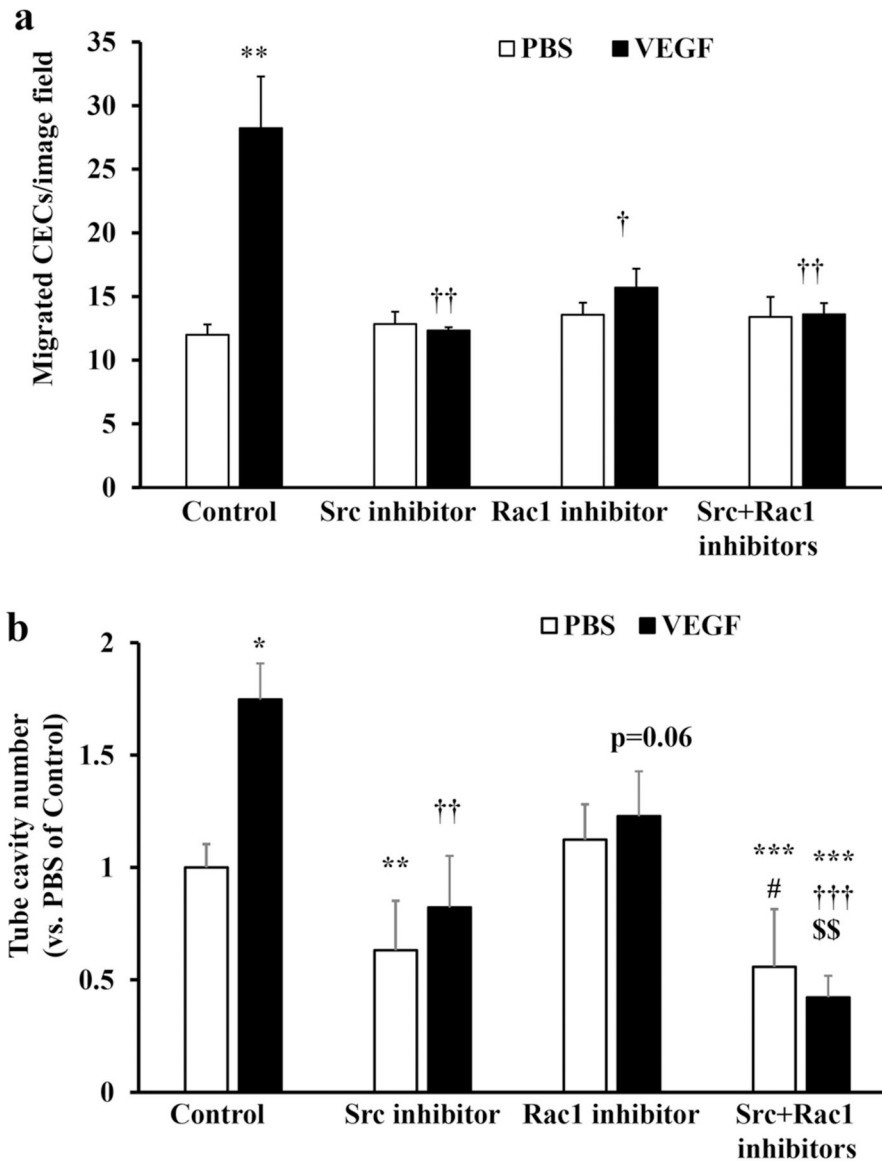


Fig. 8. Inhibition of Src or Rac1 inhibits VEGF-mediated CEC migration and tube formation. a. CEC migration and b. tube formation were performed in CECs incubated with Src inhibitor, Saracatinib (10 nM), or/and Rac1 inhibitor (50 μ M) in the presence or absence of VEGF (25 ng/ml) overnight (* p <0.05, ** p <0.01 vs. PBS of Control; p =0.06, † p <0.05, †† p <0.01, and ††† p <0.001 vs. VEGF of Control; # p <0.05 vs. PBS of Rac1 inhibitor and \$\$\$ p <0.01 vs. VEGF of Rac1 inhibitor; n =6–9 from two individual experiments).

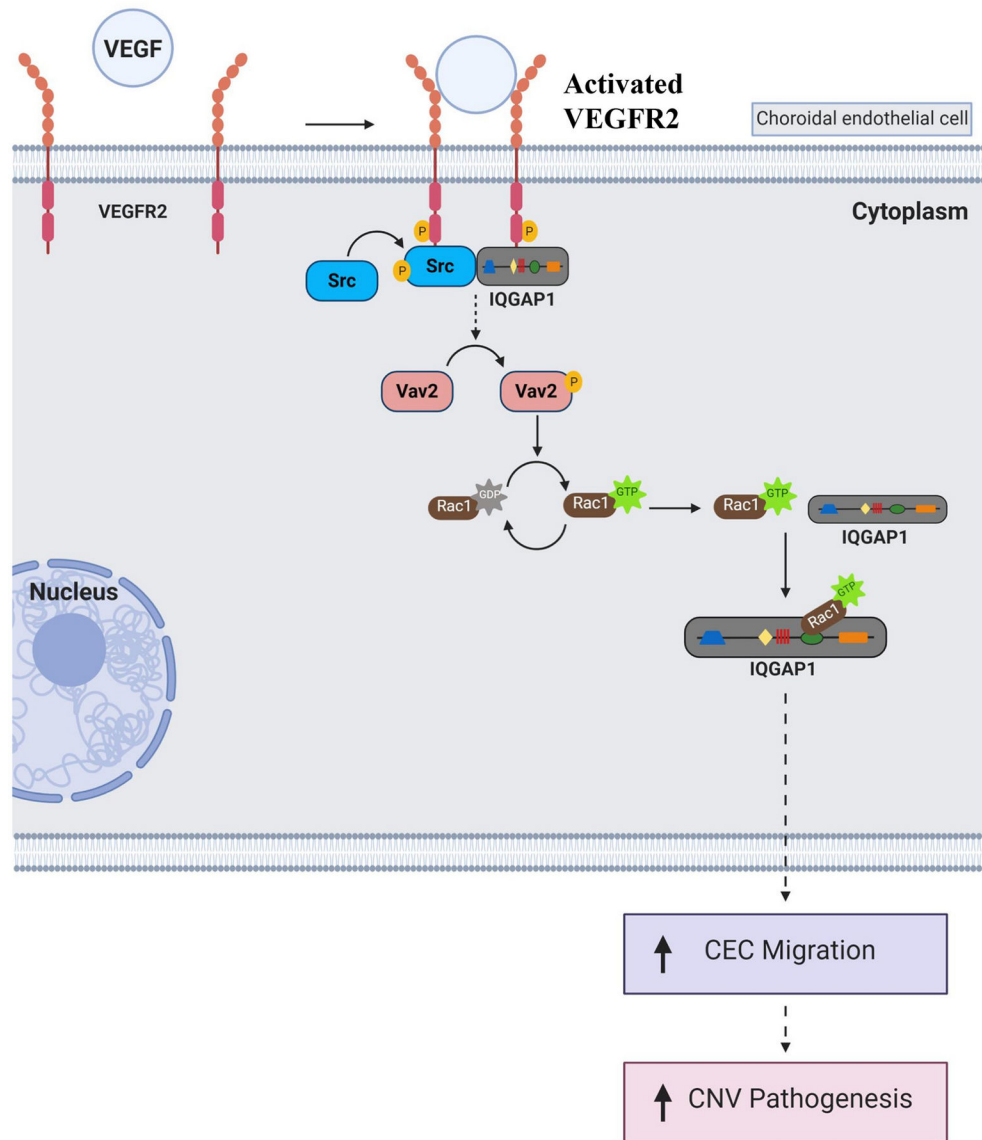


Fig. 9. Diagram of signaling pathway of IQGAP1 in regulation of VEGFR2-Src-Rac1 activation in choroidal angiogenesis.

In choroidal endothelial cell, upon binding to VEGF, VEGFR2 interacts with IQGAP1, leading to VEGFR2 activation. Activated VEGFR2 recruits Src and results in Src phosphorylation. Once Src is activated by VEGFR2 and IQGAP1, it activates Rac1 potentially involving phosphorylation of vav guanine nucleotide exchange factor 2 (Vav2), then leads to Src activation (from Rac1GDP to Rac1GTP). Once Rac1 is activated, Rac1GTP binds to IQGAP1 via GRD domain. This interaction between IQGAP1 and Rac1 maintains persistent Rac1 activation, which leads to CEC migration and CNV formation (the diagram was produced with BioRender).